Isotope-selective dissociation of diatomic molecules by terahertz optical pulses

Akira Ichihara,[1,*] Leo Matsuoka,[2] Etsuo Segawa,[3] and Keiichi Yokoyama[1]
[1]*Quantum Beam Science Center, Japan Atomic Energy Agency, Kizugawa, Kyoto 619-0215, Japan*
[2]*Graduate School of Engineering, Hiroshima University, Higashi-Hiroshima, Hiroshima 739-8527, Japan*
[3]*Graduate School of Information Sciences, Touhoku University, Sendai, Miyagi 980-8579, Japan*
(Received 24 October 2014; published 9 April 2015)

We propose a method for isotope-selective dissociation of diatomic molecules in the gas phase by using two kinds of terahertz-pulse fields. The first field consists of a train of pulses, composing a frequency comb, which excites only the selected isotope into a highly rotationally-excited state. The second field dissociates the excited molecules by further rovibrational excitations. We numerically demonstrate the applicability of the proposed scheme by molecular wave-packet computations using the lithium chlorides $^7Li^{35}Cl$ and $^7Li^{37}Cl$. Nearly 20% of the $^7Li^{37}Cl$ in the lowest rovibrational state is dissociated in a single interaction of the designed terahertz fields, while the dissociation probability is negligible in $^7Li^{35}Cl$. This scheme is expected to be applicable to the molecular ensemble whose rotational states spread in energy.

DOI: 10.1103/PhysRevA.91.043404 PACS number(s): 33.80.Gj, 31.15.xv, 33.80.Wz

I. INTRODUCTION

Terahertz (1 THz $= 10^{12}$ cycles per second) radiation is loosely defined by the frequency range of 0.1 to 10 THz [1], which corresponds to the frequency range of the one-photon pure-rotational transition of many diatomic molecules. Rapid progress of THz pulse sources has enabled the generation of intense THz pulses with peak fields of $\geqslant 10^7$ V/cm [2–4]. In recent years, molecular orientation has been studied actively with intense THz pulse fields [5–12]. Along with the generation of high-intensity fields, pulse shaping has also been attempted as well as visible and infrared lasers. For example, a THz pulse train and its comb shaped spectrum was realized by the development of new optical devices [13]. These technologies are revolutionizing the quantum control of molecular rovibrational states and its applications.

Quantum control of molecular processes has been studied in both chemistry and physics [14]. As an application of the quantum control to industry, laser isotope separation has been studied well [15–29]. The laser isotope separation is attractive because it can realize high separation efficiency with a small-scale facility [30]. The method generally utilizes the isotope shift of absorption wavelength. In these days, also the quantum interferences of wave packets generated by the broadband lasers have been playing important roles for obtaining the isotope selectivity. In 1996, Averbukh *et al.* proposed the vibrational-wave-packet isotope separation scheme [15]. They adjusted pulse timing to the revival time of the wave packet of the isotope for inducing selective ionization. Phase-locked pulses were applied by Verlet *et al.* [16]. The scheme was extended by Lindinger *et al.*, who carried out closed loop optimal control experiments [17–19]. Also, the potential by the isotope-selective molecular rotational alignment has been investigated experimentally by Fleischer *et al.* [20,21], Akagi *et al.* [22,23], and Zhdanovich *et al.* [24]. The wave-packet isotope separation has been being studied theoretically from the viewpoint of optimal control simulations to obtain the best pulse shapes [25–28]. Karczmarek *et al.* have proposed the isotope selective dissociation scheme with intense infrared fields [31].

In 2010, Yokoyama *et al.* proposed a laser isotope separation scheme applicable to diatomic molecules [32]. They utilize a train of THz pulses, which is equivalent to a THz frequency comb that exhibits regularly spaced spectral lines. By tuning the spectral frequencies of the comb to the rotational transition frequencies of the selected isotope molecule, the rotational population of the isotope is massively excited to higher states. Because the comb can induce cascading transitions between any neighboring rotational states, this scheme has a potential scalability to separate the molecular ensemble at high temperatures [33]. However, in real molecules, the spacing of rotational transition frequencies is not uniform, owing to the centrifugal distortion. To compensate for the effect of centrifugal distortion by the pulse shaping, the pulse shape in the time domain would be complicated and require a precise phase control [34].

In the present study, we simplify the pulse shape to make the experimental demonstration feasible by currently available technologies. We use two parts of a THz field which are composed of only the Fourier-transform-limited THz pulses. First, a train of a few pulses having moderately high intensity excites the selected isotope into a high rotational state. The amplitude of pulses in the train is adjusted from the viewpoint of the "gate" structure appearing in the rotational spectrum. Second, another intense THz pulse is irradiated to dissociate the molecule. The second pulse is designed to induce successive rovibrational excitations only in the molecules in highly excited states. We demonstrate its applicability by showing isotope separation of $^7Li^{35}Cl$ and $^7Li^{37}Cl$ in the initial state ($v = 0, J = 0$). Here v and J represent the vibrational and rotational quantum numbers, respectively.

This paper is structured as follows. In Sec. II, we explain the concept of the design of the THz fields for the isotope selective dissociation of LiCl. In Sec. III, we mention the computational method of wave-packet simulation. In Sec. IV, we present the results of computer simulations and discussion is given in Sec. V. Section VI contains some concluding remarks. We use atomic units $\hbar = m_e = e = 1$ in the formulation, unless explicitly stated otherwise.

*ichihara.akira@jaea.go.jp

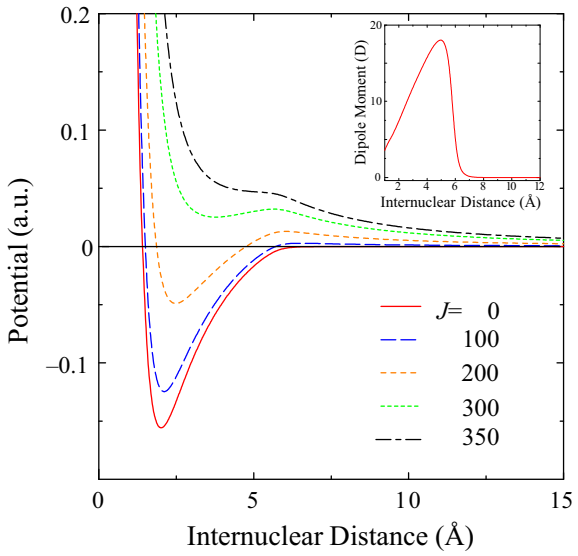

FIG. 1. (Color online) Potential energy curves of LiCl as a function of internuclear distance obtained from the *ab initio* adiabatic electronic potential [37] supplemented by centrifugal potentials. The inset is the molecular dipole moment [37] as a function of internuclear distance, which is used in Eq. (4).

II. DESIGN OF ELECTRIC FIELDS

We consider that the pulsed electric field is linearly polarized. The field $\epsilon(t)$ at time t is given by a combination of the frequency comb [$\epsilon_1(t)$ for $0 \leqslant t \leqslant t_1$] and the intense pulse field [$\epsilon_2(t)$ for $t_1 < t \leqslant t_2$] as

$$\epsilon(t) = \begin{cases} \epsilon_1(t) & (0 \leqslant t \leqslant t_1) \\ \epsilon_2(t) & (t_1 < t \leqslant t_2). \end{cases} \tag{1}$$

A. Frequency comb

We define the comb electric field by a form of a periodic δ function (Dirac comb) [35]:

$$\epsilon_1(t) = \gamma \left[1 + 2 \sum_{j=1}^{J_{\max}} \cos\{2\pi \nu_c j (t - \delta_c)\} \right], \tag{2}$$

where γ and ν_c are the parameters to determine the peak amplitude and spectral frequencies, respectively. The factor δ_c is the offset of time. It is apparent that the comb is composed of the frequency components with $\{\nu_c j; (j = 1,2,\ldots,J_{\max})\}$ which are the multiples of ν_c.

If the molecule can be treated as a rigid rotor, the rotational energy is obtained by $2\pi B J(J+1)$, where $B = 1/(2I)$ is the rotational constant and I is the moment of inertia. From this expression, the transition frequencies between neighboring rotational states are exactly given by the multiples of $2B$. Therefore, if $\nu_c = 2B$ is chosen, the cascading rotational excitation is induced by the resonant reaction. However, in real molecules, the internuclear distance is stretched by the centrifugal force (see Fig. 1). The deviation of transition frequencies from the rigid rotor model increases with the increase of J. Thus the rotational excitation by the comb is restricted by the frequency deviation due to the centrifugal distortion. To overcome this problem with keeping isotope selectivity, we adopt a moderately intense THz pulse train tolerative to the centrifugal distortion and make use of the gate region of a rotational spectrum.

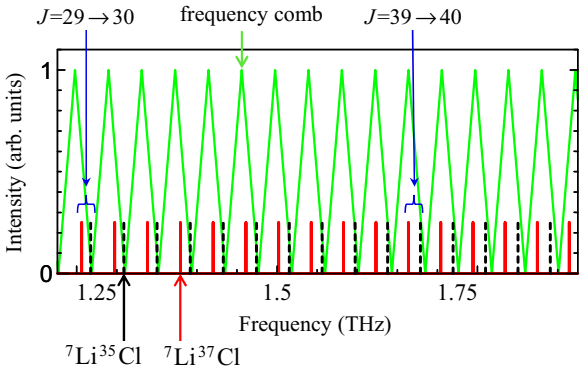

FIG. 2. (Color online) Diagram of the gate region ($30 \leqslant J \leqslant 45$) of the rotational spectrum for discriminating ^{7}Li^{35}Cl and ^{7}Li^{37}Cl, and the comb spectrum constructed by the two THz pulses for retarding ^{7}Li^{35}Cl.

The gate in our scheme means the frequency region where the discrepancy of transition frequencies between isotopes becomes the maximum. For example, the gate region between ^{7}Li^{35}Cl and ^{7}Li^{37}Cl is shown in Fig. 2. By tuning the spectral peaks of the frequency comb to the desired isotope (^{7}Li^{37}Cl), we can selectively excite it. Simultaneously, the transition frequencies of the undesired isotope will be located at the bottoms of the valleys.

The amplitudes of the pulse train is determined to maximize the isotope selection in the gate region. In our case, the amplitude was set to excite the rotational population from $J = 0$ to $J \sim 30$ in the first single pulse, in order to bring the wave front of the rotational population right below the gate region. Actually, the rotational excitation by the first pulse is quite insensitive between the isotopes; however, the following pulses induce the isotope-selective quantum interference by composing a frequency comb. In Fig. 2, the spectral shape of THz pulses for extracting ^{7}Li^{37}Cl is shown. The ν_c value was set to reproduce the ^{7}Li^{37}Cl transition frequency between $J = 39$ and 40; therefore, most transition frequencies of ^{7}Li^{35}Cl are located on valleys of the comb. In this case, ^{7}Li^{35}Cl cannot overcome the gate region owing to the destructive interference; on the other hand, ^{7}Li^{37}Cl is excited successively by the following pulses. If ^{7}Li^{35}Cl was excited above the gate by the first pulse, the following pulse would also excite it into a higher region. The amplitude of pulses is important so as not to excite the undesired isotope over the gate region in the single pulse.

Here we need to mention that the ^{7}Li^{37}Cl transition frequencies do not exactly coincide with the peak frequencies of the comb teeth. Nevertheless, a frequency comb consisting of "a few pulses" forms the teeth having a certain frequency width. These comb teeth can contain the ^{7}Li^{37}Cl transition frequencies including the effect of centrifugal distortion. (The single pulse with the duration $\sim 1/\nu_c$ produces a broad spectrum.) Thus, even though ^{7}Li^{37}Cl is not excited like the rigid rotor model, a part of ^{7}Li^{37}Cl can be transferred to a high rotational state isotope-selectively.

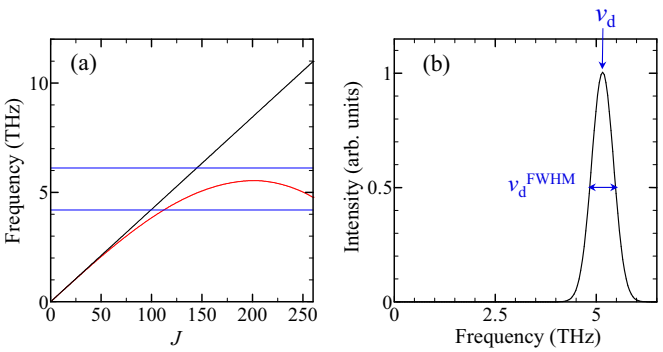

FIG. 3. (Color online) (a) Transition frequency of ^{7}Li^{37}Cl between the $(v, J) = (0, J')$ and $(0, J' + 1)$ states as a function of J. The transition frequency of the rigid rotor is shown by a straight line with the gradient $2B = 0.04222$ THz. The frequency range considered for dissociating ^{7}Li^{37}Cl is indicated by horizontal lines. (b) Intensity of the optical field for dissociating ^{7}Li^{37}Cl as a function of frequency.

B. Dissociation pulse

The selected isotope is excited to the rotational state into $J \sim 100$ by using a frequency comb. Then the highly-excited molecule is dissociated by another linearly polarized intense THz pulse. This pulse field is defined by

$$\epsilon_2(t) = A\cos\{2\pi\nu_d(t-\delta_d)\}\exp\{-(t-\delta_d)^2/2\sigma^2\}, \qquad (3)$$

where A is the peak amplitude, ν_d is the center frequency, δ_d is the delay time from the beginning of comb irradiation, and σ determines the full width at half maximum (FWHM) of the Gaussian envelope.

The pulse parameters are selected to induce successive rotational excitations from $J \sim 100$ to the dissociation limit. Figure 3(a) illustrates the transition frequency between the $(v, J) = (0, J')$ and $(0, J' + 1)$ states as a function of J. (The rovibrational energies have been evaluated by the Fourier grid Hamiltonian method [36] using an *ab initio* adiabatic electronic potential [37]. See Fig. 1 and Sec. III.) In Fig. 3(a), the transition frequency of the rigid rotor is also shown by a straight line with the gradient $2B$. The deviation between these two frequencies is remarkable in $J > 50$. The frequency exhibits the maximum at $J \sim 200$. By referring to the spectral shapes obtained from the Fourier transform of Eq. (3), the frequency range can be selected to cover the transition frequencies with $J \gtrsim 100$. Figure 3(b) shows the spectral intensity of the THz pulse to induce the successive rotational excitation to the dissociation. From ν_d^{FWHM} in Fig. 3(b), the parameter σ in Eq. (3) is obtained by using the relation $\sigma = (\sqrt{\ln 2}/\pi)/\nu_d^{FWHM}$ assuming the Fourier-transform-limited pulse with the Gaussian envelope.

In LiCl molecules, moreover, the transition frequency between $(v, J) = (0, J')$ and $(1, J' - 1)$ is smaller than that between $(0, J')$ and $(0, J' + 1)$, if $J \geqslant 200$. Thus the dissociation should be brought about through both the rotational and vibrational excitations by this pulse.

C. Field parameters

Table I indicates parameter values of the THz fields. We employ the frequency comb consisting of four pulses to excite the rotational state of ^{7}Li^{37}Cl isotope-selectively. The frequency parameter ν_c in Eq. (2) was selected to 0.04160 THz. This value was chosen to produce the transition frequency of ^{7}Li^{37}Cl between $J = 39$ and 40. The derived pulse interval is $T = 1/\nu_c = 2.404 \times 10^{-11}$ s. To excite the rotational state into $J \geqslant 100$, $J_{max} = 120$ was used. The factor δ_c was set to $1.202 \times 10^{-11}\text{s} = 1/(2\nu_c) = 0.5T$. Thus the four pulses are introduced at time $t = 0.5T, 1.5T, 2.5T$, and $3.5T$. The γ value was chosen to transfer the rotational state J from 0 to ~30 by the first pulse. We selected $\gamma = 5.62 \times 10^4$ V/cm, which provides the peak height of $(2J_{max} + 1)\gamma = 1.35 \times 10^7$ V/cm. The resulting pulse train is shown in Fig. 4(a).

TABLE I. Field parameters.

Symbol	Value	Unit
γ	5.62×10^4	V/cm
ν_c	0.04160	THz
δ_c	1.202×10^{-11}	s
J_{max}	120	
A	6.17×10^7	V/cm
ν_d	5.16	THz
δ_d	1.082×10^{-10}	s
σ	4.15×10^{-13}	s

The pulse for dissociating ^{7}Li^{37}Cl is given in Eq. (3). The values of frequency parameters ν_d and ν_d^{FWHM} were chosen to cover the ^{7}Li^{37}Cl transition frequencies in the range $100 \leqslant J \leqslant 200$ in Fig. 3. We estimated them as $\nu_d = 5.16$ and $\nu_d^{FWHM} = 0.639$ THz, respectively. The value of $\sigma = 4.15 \times 10^{-13}$ s was evaluated from ν_d^{FWHM}. The factor δ_d was set to $1.082 \times 10^{-10}\text{s} = 4.5T$. We selected

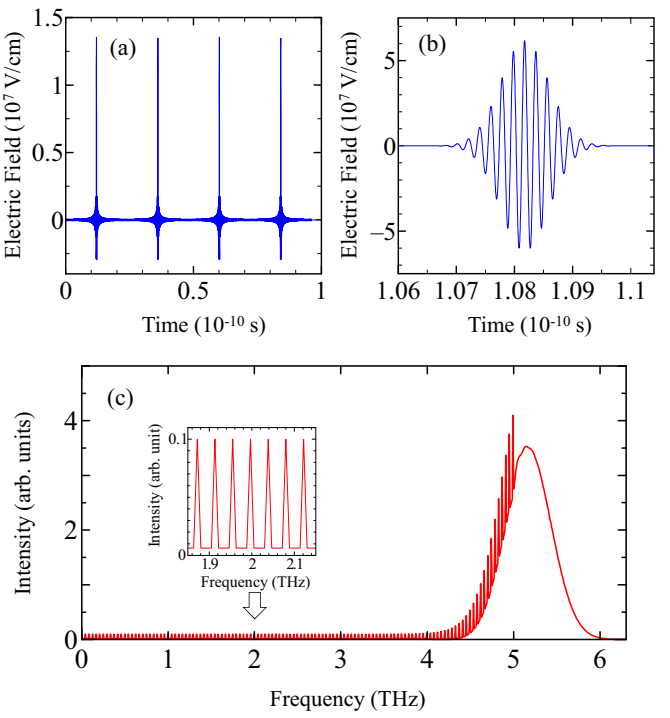

FIG. 4. (Color online) (a) The frequency comb field as a function of time. (b) The pulse field for dissociating ^{7}Li^{37}Cl as a function of time. (c) Intensity of the combined pulse fields as a function of frequency. The inset is the enlargement of the frequency comb.

$A = 6.17 \times 10^7$ V/cm (0.012 a.u.) to dissociate ^{7}Li^{37}Cl and not to ionize the molecules. The pulse field applied is shown in Fig. 4(b).

In Fig. 4(c), the field intensity is shown as a function of frequency. The spectra are the sum of the frequency comb which consists of 121 teeth and the spectrum which takes a Gaussian distribution for dissociating ^{7}Li^{37}Cl. We observe the overlap of two kinds of spectra between 4 to 5 THz. The inset is the enlargement of the frequency comb.

III. COMPUTATIONAL METHOD

To demonstrate the applicability of our method, we dissociate ^{7}Li^{37}Cl isotope-selectively in the proposed pulse fields. The interaction $\hat{V}(t)$ between the pulse and the molecule is given by the field-dipole interaction,

$$\hat{V}(R,\theta,t) = -\epsilon(t)\cdot\mu(R)\cos\theta, \tag{4}$$

where $\epsilon(t)$ is the pulse field, $\mu(R)$ is the molecular dipole moment at the internuclear distance R, and θ is the angle between the pulse field and the molecular axis.

The time evolution of molecular rovibrational states was computed using the wave-packet method with the split-operator technique [38,39]. In this method, the initial wave function is transformed using the short-time (Δt) evolution propagator $\hat{U}(R,\theta,t+\Delta t)$ which is expressed by

$$\begin{aligned}\hat{U}(R,\theta,t+\Delta t) &= e^{-i\Delta t\{\hat{T}_R+\hat{T}_\theta+\hat{V}_0(R)+\hat{V}(R,\theta,t)\}}\\ &\approx e^{-i\Delta t\hat{T}_R/2}e^{-i\Delta t\hat{T}_\theta/2}e^{-i\Delta t\{\hat{V}_0(R)+\hat{V}(R,\theta,t)\}}\\ &\quad\times e^{-i\Delta t\hat{T}_\theta/2}e^{-i\Delta t\hat{T}_R/2},\end{aligned} \tag{5}$$

where $\hat{T}_R$ and $\hat{T}_\theta$ are kinetic energy operators of the radial and angular parts, respectively. $\hat{V}_0(R)$ is the adiabatic potential in the ground electronic state. The time evolution is computed by repeatedly operating $\hat{U}$. In the calculation, $\hat{T}_R$ is transformed between the coordinate (R) space and momentum space using the fast Fourier transform (FFT) technique [40]. Similarly, $\hat{T}_\theta$ is transformed between the coordinate (θ) space and polynomial (Legendre polynomials) space using the discrete variable representation (DVR) [41]. Each transformation of $\hat{T}_R$ or $\hat{T}_\theta$ is performed by keeping other variable fixed. In this study, the time evolution was carried out with the time step $\Delta t = 5\times10^{-6}T \sim 10^{-5}T$.

The molecular wave packet is computed in the range of internuclear distance between $R_{\min} = 10^{-10}$ (1 Å) and $R_{\max} = 1.5\times10^{-9}$ m (15 Å) by using the *ab initio* adiabatic potential and the dipole moment taken from [37]. The employed adiabatic potential and dipole moment are shown in Fig. 1. Since the energy difference 0.15571 a.u. (hartree) between the potential minimum at $R = 2.0094$ Å and the potential at $R_{\max}$ is only 1.4×10^{-4}% (2.2×10^{-7} a.u.) smaller than that calculated with $R = 100$ Å [37], we selected $R_{\max}$ for the criterion of dissociation. In order to extract the probability amplitude of each rovibrational state from the wave packet, the rovibrational energy E_{vJ} and function $\phi_{vJ}(R)$ in the state (v,J) were evaluated by the Fourier grid Hamiltonian method [36] with 1024 radial grid points. The rovibrational functions were calculated one by one by taking into account the centrifugal potential (see Fig. 1). The evaluated rotational constant B in the $(v,J) = (0,0)$ state is 0.02111 THz.

In calculating the wave packet, 1024 radial and 128 angular grid points were used for the frequency comb ($0 \leqslant t \leqslant t_1 = 4T$) irradiation. Also, 1024 radial and 336 angular grids were employed for the dissociation ($4T < t \leqslant t_2 = 5T$) process. In the DVR method, the highest rotational quantum number is equal to the number of angular grids minus 1. Since the adiabatic potential is repulsive in $J \geqslant 335$ and no bound and quasibound states are formed there, we utilized 336 angular grids in the calculation of the dissociation process (see Fig. 1). The initial wave packet on the 1024 radial and 336 angular grids was formed employing the probability amplitudes of rovibrational states obtained from the final wave packet on the 1024 radial and 128 angular grids.

In order to estimate the dissociation probability, the wave-packet component reaching up to $R_{\max}$ was eliminated using a sinusoidal damping function which operates on the last five grid points from $R_{\max}$ [34,42]. The dissociation probability was estimated by the sum of the eliminated components.

Also, in order to assess the numerical accuracy, the probability amplitudes C_{vJ} were evaluated by solving the coupled-channel equations in the interaction picture [43],

$$\begin{aligned}i\frac{d}{dt}C_{vJ} &= -\epsilon(t)\sum_{v'}\{V_{vJ,v'J-1}C_{v'J-1}(t)\\ &\quad + V_{vJ,v'J+1}C_{v'J+1}(t)\},\end{aligned} \tag{6}$$

with [44]

$$\begin{aligned}V_{vJ,v'J-1} &= \frac{Je^{i(E_{vJ}-E_{v'J-1})t}}{\sqrt{(2J-1)(2J+1)}}\\ &\quad\times\int\phi_{vJ}(R)\mu(R)\phi_{v'J-1}(R)dR,\end{aligned} \tag{7}$$

$$\begin{aligned}V_{vJ,v'J+1} &= \frac{(J+1)e^{i(E_{vJ}-E_{v'J+1})t}}{\sqrt{(2J+1)(2J+3)}}\\ &\quad\times\int\phi_{vJ}(R)\mu(R)\phi_{v'J+1}(R)dR.\end{aligned} \tag{8}$$

From Eq. (6), both the ^{7}Li^{35}Cl and ^{7}Li^{37}Cl rotational distributions were evaluated in $0 \leqslant t \leqslant 4T$. The population distributions were obtained by the fourth order Runge-Kutta computations [40] with 3 vibrational ($v = 0$ to 2) and 180 rotational ($J = 0$ to 179) states. We confirmed that the difference of populations between the coupled-channel and wave-packet methods was within 10^{-3} at $4T$. Moreover, in ^{7}Li^{35}Cl, the population was computed up to $5T$. The deviation from the wave-packet calculation was 3×10^{-3} or less at $5T$. It was confirmed that the rotational distributions from the two computational methods overlap with each other and the difference is almost invisible in Fig. 5.

IV. RESULTS

Figure 5 shows the rotational population distributions of ^{7}Li^{35}Cl and ^{7}Li^{37}Cl excited by the optical pulses in Fig. 4. Initially, these molecules are in the $(v,J) = (0,0)$ state. Each figure from Figs. 5(a) to 5(e) shows the rotational distribution of ^{7}Li^{35}Cl obtained after the first to fourth comb pulse [Figs. 5(a)–5(d)] and the dissociating pulse [Fig. 5(e)]

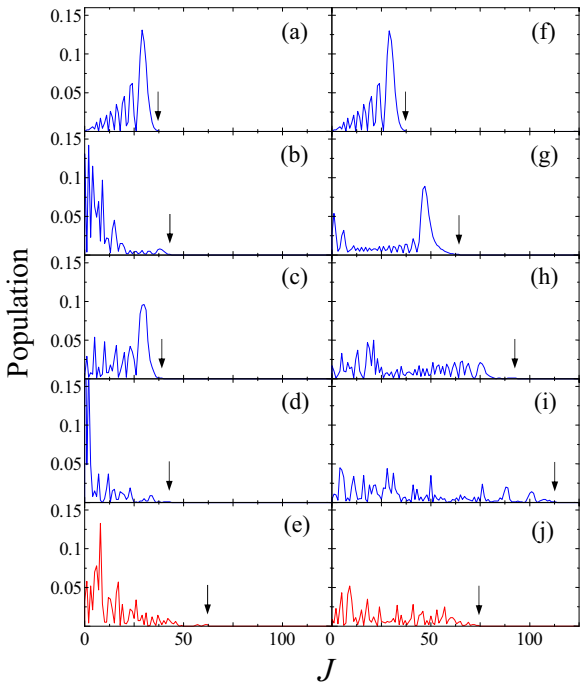

FIG. 5. (Color online) Rotational population distributions of (a)–(e) ^{7}Li^{35}Cl and (f)–(j) ^{7}Li^{37}Cl obtained by the optical pulses in Fig. 4. The molecules are in the $(v = 0, J = 0)$ state, initially. The figures from (a) to (e) and from (f) to (j) are the distributions evaluated at time T,$2T$,$3T$,$4T$, and $5T$ ($T = 2.404 \times 10^{-11}$s), respectively. The highest J states having the population $\geqslant 10^{-3}$ are indicated by arrows.

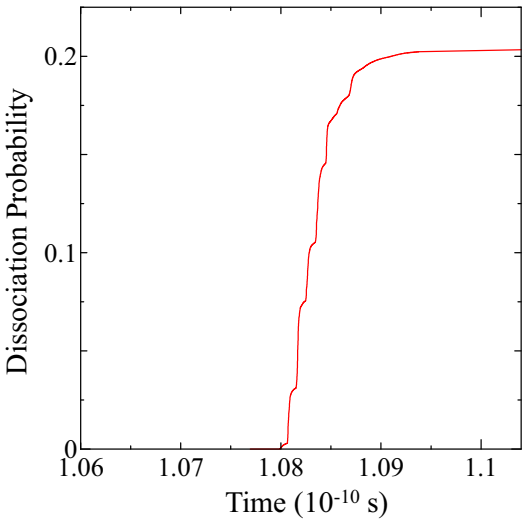

FIG. 6. (Color online) Dissociation probability of ^{7}Li^{37}Cl as a function of time.

irradiation. Figures 5(f)–5(j) are the corresponding results for ^{7}Li^{37}Cl. The highest J states having the population $\geqslant 10^{-3}$ are indicated by arrows.

In Figs. 5(a) and 5(f), the same distributions are obtained in ^{7}Li^{35}Cl and ^{7}Li^{37}Cl. The remarkable difference appears between Figs. 5(b) and 5(g). The ^{7}Li^{35}Cl molecule can not be excited beyond $J \sim 40$ by the destructive interference over the gate region as depicted in Fig. 2. Thus the ^{7}Li^{35}Cl distribution is reflected back to lower states. In Figs. 5(f)–5(i), ^{7}Li^{37}Cl is excited gradually up to $J \sim 110$ by the frequency comb. In Figs. 5(b)–5(d) the distributions of ^{7}Li^{35}Cl are restricted to $J \lesssim 40$.

In the wave-packet simulation, ^{7}Li^{37}Cl in a high J state is dissociated by the pulse shown in Fig. 4(b). The dissociation probability of 20.4% was obtained. It can be seen from Fig. 5(j) that ^{7}Li^{37}Cl in $J \geqslant 70$ is dissociated. In ^{7}Li^{35}Cl, the dissociation probability was 0.004%. Figure 6 indicates the time dependence of the ^{7}Li^{37}Cl dissociation probability. From Figs. 4(b) and 6, we can observe that ^{7}Li^{37}Cl is mainly dissociated in the time between 1.08 and 1.09 $\times 10^{-10}$ s ($4.49T \leqslant t \leqslant 4.53T$) around the pulse peak.

We also evaluated the influence of vibrational excitation in the processes. In the frequency comb irradiation, the probability of vibrational excitation was less than 0.1% at $t = 4T$ in both ^{7}Li^{35}Cl and ^{7}Li^{37}Cl [34]. When dissociating ^{7}Li^{37}Cl, vibrational states with the population $\geqslant 10^{-3}$ were formed up to $v \sim 30$. At the pulse peak of $4.5T$, about 30% was vibrationally excited. In ^{7}Li^{35}Cl, the population in the $v = 1$ state was 5×10^{-3} at $5T$, and the vibrational excitation to $v \geqslant 2$ was negligible.

V. DISCUSSION

In this study, we numerically demonstrated the isotope separation of LiCl using two kinds of THz pulse fields. The obtained dissociation probability of the desired isotope was 20.4%, and that of the undesired isotope was 0.004%. We obtained quite high isotope selectivity for diatomic molecules. Here, we discuss ionization, which is a potential obstacle and not included in our simulation explicitly. However, the effect is thought to be negligible. We evaluated the ionization rate as a function of field intensity using the Ammosov-Delone-Krainov (ADK) formula given by Brichta *et al.* [45,46]. Also, the ionization rate of LiCl which has the ionization potential 10.01 eV [47] was assessed referring to the works by Otobe *et al.* [48,49]. It was estimated that the ionization is negligible if the peak intensity is less than 2×10^{13} W/cm^2($\sim 1.2 \times 10^8$ V/cm), which is four times as high as the intensity of the dissociation pulse in our calculation.

Vibrational excitation in the frequency comb would make an influence to the selection of isotopes. However, the vibrational excitation was negligibly small in our calculation. We think there are three reasons for this result. First, the rotational transition frequencies taken into account are lower than the transition frequencies required for the vibrational excitation. The highest rotational transition frequency of ^{7}Li^{37}Cl [between the $(v, J) = (0,119)$ and $(0,120)$ states] is 4.41 THz, while the lowest vibrational transition frequency [between the $(0,120)$ and $(1,119)$ states] is 11.9 THz. Second, the transition dipole moment between (v, J) and $(v+1, J \pm 1)$ should be smaller than that for pure rotational transition between (v, J) and $(v, J \pm 1)$ [37]. Finally, the frequency selective interference in the frequency comb must be working not only for the rotational excitation but also for the vibrational excitation.

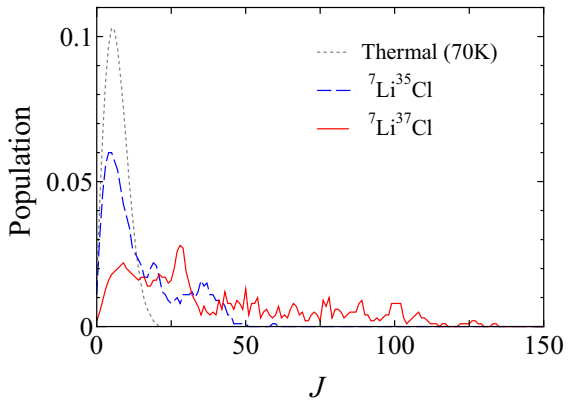

FIG. 7. (Color online) Population transfer of the ^{7}Li^{35}Cl and ^{7}Li^{37}Cl ensembles at 70 K induced by the THz frequency comb in Fig. 4(a). The rotational distributions at $4T$ are shown.

In this study, the simulation was performed using the molecule in the ground state ($v = 0, J = 0$). However, the THz frequency comb is expected to realize the rotational heating of the molecular ensemble which is mentioned in the previous reports [32,33]. Actually, we have numerically evaluated the population transfer of the LiCl ensembles that take the thermal (Maxwellian) distribution at 70 K for which molecular beam experiments are thought to be possible [50]. The population transfer from 231 initial rotational states ($0 \leqslant J \leqslant 20, J \geqslant |M|$, M: magnetic quantum number) was evaluated by solving the coupled equation of Eq. (6) using Eqs. (7) and (8) where the factors for angular momentum transfer were altered from $J/\sqrt{(2J-1)(2J+1)}$ to $\sqrt{J^2-M^2}/\sqrt{(2J-1)(2J+1)}$ and from $(J+1)/\sqrt{(2J+1)(2J+3)}$ to $\sqrt{(J+1)^2-M^2}/\sqrt{(2J+1)(2J+3)}$, respectively. The obtained result is shown in Fig. 7. By using the proposed frequency comb, ^{7}Li^{37}Cl is excited beyond the gate region $J \sim 40$, and the excitation of ^{7}Li^{35}Cl is interrupted near this region. The excitation probability into the $J > 70$ states was 20.5% for ^{7}Li^{37}Cl and 0.5% for ^{7}Li^{35}Cl. These highly excited molecules would be dissociated by the second pulse.

It is pointed out that Karczmarek *et al.* have proposed the scheme for isotope-selective dissociation prior to our study [31]. In their scheme, strong infrared fields are applied to molecules and dissociation is brought about by the field-induced dipole interaction. Their simulation for Cl_2 molecules showed that 8.5% of $^{37}Cl_2$ was broken and the dissociation of $^{35}Cl_2$ was completely suppressed. Our result for the ($v = 0, J = 0$) initial state is comparable to their work. The present method may be more suitable to avoid ionization in polar molecules. We provide an alternative option to dissociate molecules isotope-selectively by using THz pulses.

VI. SUMMARY AND CONCLUDING REMARKS

We proposed a method to dissociate diatomic molecules isotope-selectively by using the THz pulse fields. We demonstrated the applicability of our method using ^{7}Li^{35}Cl and ^{7}Li^{37}Cl molecules in the lowest rovibrational state. About 20% of ^{7}Li^{37}Cl was dissociated isotope-selectively. We expect the proposed method is applicable to dissociate other diatomic molecules.

In this method, the rotational states of molecules are excited by the frequency comb composed of a few pulses. The first pulse transfers the rotational states into the gate region where the transition frequencies of the isotopes appear near the halfway points of the frequency intervals with each other. The timing of the second pulse is determined to induce isotope-selective quantum interference by adjusting the spectral shape of the frequency comb composed by multiple pulses. After the frequency comb irradiation, the molecules are exposed to another pulse field. This pulse is designed to dissociate excited molecules via further successive rotational excitations. Its spectral frequency range is chosen to include the highest rotational transition frequency of the selected isotope molecule. Since we do not make any specific assumption in diatomic molecules, the proposed method should be applicable to diatomic molecules other than LiCl. By employing two kinds of THz fields, the molecules can be dissociated isotope-selectively.

The present study shows that the precise phase control of THz fields is not necessary to induce the isotope-selective dissociation through the rotational cascade which was introduced in our previous work. The considered THz optical fields will be realized in the near future. The present simulation will give parameter information to the experimental demonstration of isotope separation by the THz optical pulses.

ACKNOWLEDGMENTS

The authors are grateful to Dr. Y. Kurosaki, who provided numerical data of the LiCl adiabatic potential and dipole moment. This work was supported by JSPS KAKENHI Grant No. 26420875.

[1] B. Ferguson and X.-C. Zhang, Nat. Mater. **1**, 26 (2002).
[2] A. Sell, A. Leitenstorfer, and R. Huber, Opt. Lett. **33**, 2767 (2008).
[3] D. Daranciang, J. Goodfellow, M. Fuchs, H. Wen, S. Ghimire, D. A. Reis, H. Loos, A. S. Fisher, and A. M. Lindenberg, Appl. Phys. Lett. **99**, 141117 (2011).
[4] M. Clerici, M. Peccianti, B. E. Schmidt, L. Caspani, M. Shalaby, M. Giguère, A. Lotti, A. Couairon, F. Légaré, T. Ozaki, D. Faccio, and R. Morandotti, Phys. Rev. Lett. **110**, 253901 (2013).
[5] C.-C. Shu, K.-J. Yuan, W.-H. Hu, and S.-L. Cong, J. Chem. Phys. **132**, 244311 (2010).
[6] S. Fleischer, Y. Zhou, R. W. Field, and K. A. Nelson, Phys. Rev. Lett. **107**, 163603 (2011).
[7] S. Fleischer, R. W. Field, and K. A. Nelson, Phys. Rev. Lett. **109**, 123603 (2012).
[8] J. Ortigoso, J. Chem. Phys. **137**, 044303 (2012).
[9] S.-L. Liao, T.-S. Ho, H. Rabitz, and Shih-I. Chu, Phys. Rev. A **87**, 013429 (2013).

[10] K. Kitano, N. Ishii, N. Kanda, Y. Matsumoto, T. Kanai, M. Kuwata-Gonokami, and J. Itatani, Phys. Rev. A **88**, 061405 (2013).
[11] Z.-Y. Zhao, Y.-C. Han, Y. Huang, and S.-L. Cong, J. Chem. Phys. **139**, 044305 (2013).
[12] M. Yoshida and Y. Ohtsuki, Phys. Rev. A **90**, 013415 (2014).
[13] M. Tsubouchi and T. Kumada, Opt. Express **20**, 28500 (2012).
[14] M. Shapiro and P. Brumer, *Quantum Control of Molecular Processes* (Wiley-VCH, Weinheim, 2012).
[15] I. Sh. Averbukh, M. J. J. Vrakking, D. M. Villeneuve, and A. Stolow, Phys. Rev. Lett. **77**, 3518 (1996).
[16] J. R. R. Verlet, V. G. Stavros, and H. H. Fielding, Phys. Rev. A **65**, 032504 (2002).
[17] A. Lindinger, C. Lupulescu, M. Plewicki, F. Vetter, A. Merli, S. M. Weber, and L. Wöste, Phys. Rev. Lett. **93**, 033001 (2004).
[18] A. Lindinger, C. Lupulescu, F. Vetter, M. Plewicki, S. M. Weber, A. Merli, and L. Wöste, J. Chem. Phys. **122**, 024312 (2005).
[19] A. Lindinger, A. Merli, M. Plewicki, F. Vetter, S. M. Weber, and L. Wöste, Chem. Phys. Lett. **413**, 315 (2005).
[20] S. Fleischer, I. Sh. Averbukh, and Y. Prior, Phys. Rev. A **74**, 041403 (2006).
[21] S. Fleischer, I. Sh. Averbukh, and Y. Prior, Phys. Rev. Lett. **99**, 093002 (2007).
[22] H. Akagi, H. Ohba, K. Yokoyama, A. Yokoyama, K. Egashira, and Y. Fujimura, Appl. Phys. B **95**, 17 (2009).
[23] H. Akagi, T. Kasajima, T. Kumada, R. Itakura, A. Yokoyama, H. Hasegawa, and Y. Ohshima, Appl. Phys. B **109**, 75 (2012).
[24] S. Zhdanovich, C. Bloomquist, J. Floß, I. Sh. Averbukh, J. W. Hepburn, and V. Milner, Phys. Rev. Lett. **109**, 043003 (2012).
[25] M. Leibscher and I. Sh. Averbukh, Phys. Rev. A **63**, 043407 (2001).
[26] B. S.-Bung, V. B.-Koutecký, F. Sauer, S. M. Weber, L. Wöste, and A. Lindinger, J. Chem. Phys. **125**, 214310 (2006).
[27] Y. Ohtsuki and Y. Fujimura, Chem. Phys. **338**, 285 (2007).
[28] B. S.-Bung, Chem. Phys. **343**, 340 (2008).
[29] Y. Kurosaki, H. Akagi, and K. Yokoyama, Phys. Rev. A **90**, 043407 (2014).
[30] V. S. Letokhov, Nature (London) **277**, 605 (1979).
[31] J. Karczmarek, J. Wright, P. Corkum, and M. Ivanov, Phys. Rev. Lett. **82**, 3420 (1999).
[32] K. Yokoyama, L. Matsuoka, T. Kasajima, M. Tsubouchi, and A. Yokoyama, in *Advances in Intense Laser Science and Photonics*, edited J. Lee *et al.* (Publishing House for Science and Technology, Hanoi, 2010), pp. 113–119.
[33] L. Matsuoka, A. Ichihara, M. Hashimoto, and K. Yokoyama, Proceedings of the International Conference Toward and Over the Fukushima Daiichi Accident (GLOBAL 2011), Makuhari, Japan, 2011, Paper No. 392063 (CD-ROM).
[34] A. Ichihara, L. Matsuoka, Y. Kurosaki, and K. Yokoyama, JPS Conf. Proc. **1**, 013093 (2014).
[35] R. Blümel, S. Fishman, and U. Smilansky, J. Chem. Phys. **84**, 2604 (1986).
[36] C. C. Marston and G. G. Balint-Kurti, J. Chem. Phys. **91**, 3571 (1989).
[37] Y. Kurosaki and K. Yokoyama, J. Chem. Phys. **137**, 064305 (2012).
[38] M. D. Feit, J. A. Fleck Jr., and A. Steiger, J. Comp. Phys. **47**, 412 (1982).
[39] K.-J. Yuan, Z. Sun, S.-L. Cong, and N. Lou, Phys. Rev. A **74**, 043421 (2006).
[40] W. H. Press, S. A. Teukolsky, W. T. Vetterling, and B. P. Flannery, *Numerical Recipes in Fortran 77*, 2nd ed. (Cambridge University Press, New York, 1992).
[41] J. C. Light, I. P. Hamilton, and J. V. Lill, J. Chem. Phys. **82**, 1400 (1985).
[42] S. Mahapatra and N. Sathyamurthy, J. Chem. Soc., Faraday Trans. **93**, 773 (1997).
[43] P. A. M. Dirac, *The Principles of Quantum Mechanics*, 4th ed. (Clarendon, Oxford, 1958).
[44] M. E. Rose, *Elementary Theory of Angular Momentum* (Wiley, New York, 1957).
[45] M. V. Ammosov, N. B. Delone, and V. P. Krainov, Sov. Phys. JETP **64**, 1191 (1986).
[46] J. P. Brichta, W.-K. Liu, A. A. Zaidi, A. Trottier, and J. H. Sanderson, J. Phys. B **39**, 3769 (2006).
[47] C.-G. Zhan, J. A. Nichols, and D. A. Dixon, J. Phys. Chem. A **107**, 4184 (2003).
[48] T. Otobe, K. Yabana, and J.-I. Iwata, Phys. Rev. A **69**, 053404 (2004).
[49] T. Otobe and K. Yabana, Phys. Rev. A **75**, 062507 (2007).
[50] C. R. Wu, J. B. Crooks, S.-C. Yang, K. R. Way, and W. C. Stwalley, Rev. Sci. Instrum. **49**, 380 (1978).